

Storm-induced upwelling of high $p\text{CO}_2$ waters onto the continental shelf of the western Arctic Ocean and implications for carbonate mineral saturation states

Jeremy T. Mathis,¹ Robert S. Pickart,² Robert H. Byrne,³ Craig L. McNeil,⁴ G. W. K. Moore,⁵ Laurie W. Juranek,⁶ Xuewu Liu,³ Jian Ma,³ Regina A. Easley,³ Matthew M. Elliot,³ Jessica N. Cross,¹ Stacey C. Reisdorph,¹ Frank Bahr,² Jamie Morison,⁴ Trina Lichendorf,⁴ and Richard A. Feely⁷

Received 2 March 2012; accepted 7 March 2012; published 11 April 2012.

[1] The carbon system of the western Arctic Ocean is undergoing a rapid transition as sea ice extent and thickness decline. These processes are dynamically forcing the region, with unknown consequences for CO_2 fluxes and carbonate mineral saturation states, particularly in the coastal regions where sensitive ecosystems are already under threat from multiple stressors. In October 2011, persistent wind-driven upwelling occurred in open water along the continental shelf of the Beaufort Sea in the western Arctic Ocean. During this time, cold ($< -1.2^\circ\text{C}$), salty (> 32.4) halocline water—supersaturated with respect to atmospheric CO_2 ($p\text{CO}_2 > 550 \mu\text{atm}$) and undersaturated in aragonite ($\Omega_{\text{aragonite}} < 1.0$) was transported onto the Beaufort shelf. A single 10-day event led to the outgassing of 0.18–0.54 Tg-C and caused aragonite undersaturations throughout the water column over the shelf. If we assume a conservative estimate of four such upwelling events each year, then the annual flux to the atmosphere would be 0.72–2.16 Tg-C, which is approximately the total annual sink of CO_2 in the Beaufort Sea from primary production. Although a natural process, these upwelling events have likely been exacerbated in recent years by declining sea ice cover and changing atmospheric conditions in the region, and could have significant impacts on regional carbon budgets. As sea ice retreat continues and storms increase in frequency and intensity, further outgassing events and the expansion of waters that are undersaturated in carbonate minerals over the shelf are probable. **Citation:** Mathis, J. T., et al. (2012), Storm-induced upwelling of high $p\text{CO}_2$ waters onto the continental shelf of the western Arctic Ocean and implications for carbonate mineral saturation states, *Geophys. Res. Lett.*, 39, L07606, doi:10.1029/2012GL051574.

¹School of Fisheries and Ocean Sciences, University of Alaska Fairbanks, Fairbanks, Alaska, USA.

²Woods Hole Oceanographic Institution, Woods Hole, Massachusetts, USA.

³College of Marine Science, University of South Florida, St. Petersburg, Florida, USA.

⁴Applied Physics Laboratory, University of Washington, Seattle, Washington, USA.

⁵Department of Physics, University of Toronto, Toronto, Ontario, Canada.

⁶College of Oceanic and Atmospheric Sciences, Oregon State University, Corvallis, Oregon, USA.

⁷Pacific Marine Environmental Laboratory, Seattle, Washington, USA.

1. Introduction

[2] The continental shelves of the western Arctic Ocean play an important and likely increasing role in the global carbon dioxide (CO_2) cycle through complex and poorly understood interactions with sea ice, ocean and atmospheric circulation, and terrestrial processes [e.g., *Bates et al.*, 2011]. Recent studies in this region have shown significant warming of the atmosphere [e.g., *Serreze and Francis*, 2006] coupled with rapidly declining sea ice extent and thickness [*Wang and Overland*, 2009] and increased storm activity [*Zhang et al.*, 2004; *Sorteberg and Walsh*, 2008]. Over the next few decades as environmental conditions change rapidly and anthropogenic CO_2 continues to accumulate in the ocean [i.e., *Sabine et al.*, 2004], enhancing ocean acidification (OA) in the western Arctic [i.e., *Bates et al.*, 2011], the marine carbon cycle in the region will likely enter a highly dynamic state.

[3] The Beaufort Sea shelf (Figure S1 in the auxiliary material) is relatively narrow with a limited physical supply of nutrients [*Carmack and Wassmann*, 2006; *Macdonald et al.*, 2010], although it does support a diverse array of both benthic and pelagic organisms [*Carmack and Macdonald*, 2002].¹ Rates of phytoplankton primary production over the shelf have been estimated at $\sim 6\text{--}12 \text{ g C m}^{-2} \text{ yr}^{-1}$ [*Macdonald et al.*, 2010; *Anderson and Kaltin*, 2001], compared to $\geq 300 \text{ g C m}^2 \text{ yr}^{-1}$ [i.e., *Mathis et al.*, 2009; *Macdonald et al.*, 2010] in the highly productive Chukchi Sea to the west. The high rate of primary production in the Chukchi Sea makes it a strong sink for atmospheric CO_2 , taking up as much as $90 \text{ mmol CO}_2 \text{ m}^{-2} \text{ d}^{-1}$ or $11\text{--}53 \text{ Tg C yr}^{-1}$ [*Bates et al.*, 2011]. In contrast, the Beaufort Sea is likely a neutral or very weak sink ($2\text{--}3 \text{ Tg C yr}^{-1}$) for atmospheric CO_2 , and may at times be an atmospheric source of CO_2 due to high rates of coastal erosion and remineralization of riverine discharge of organic matter [*Carmack and Macdonald*, 2002].

[4] The physical circulation in this region is dominated by a boundary current [*Nikolopoulos et al.*, 2009] along the Beaufort shelfbreak that, in the mean, flows to the east (Figure S1). The current carries Pacific-origin waters that have been modified by physical and biogeochemical processes while transiting through the Chukchi Sea [*Weingartner et al.*, 1998; *Mathis et al.*, 2007]. At times, the boundary current

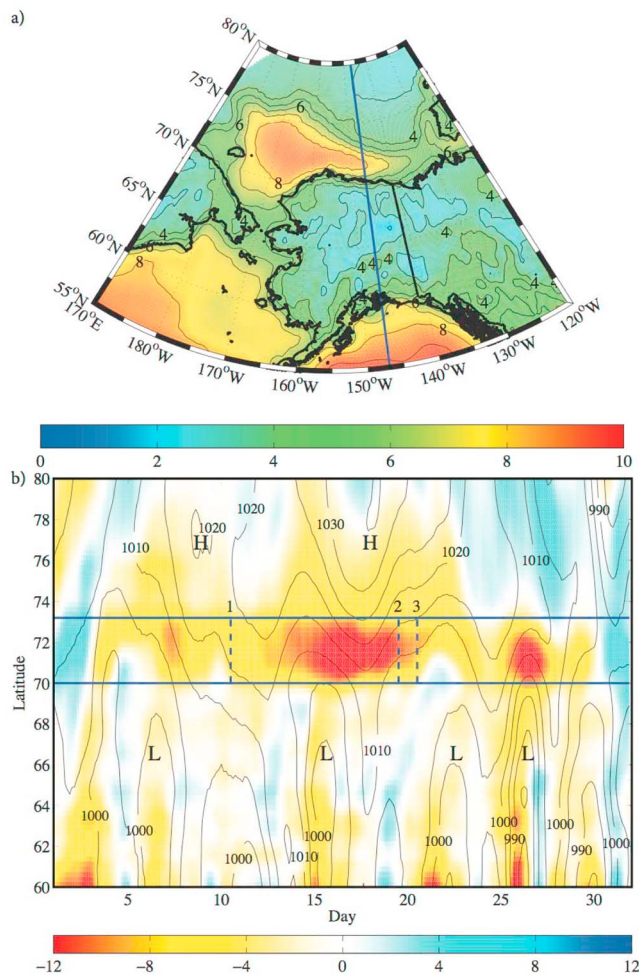


Figure 1. Atmospheric conditions over the Beaufort Sea during October 2011. (a) The monthly mean 10 m wind speed (contours and color, m s^{-1}). (b) The Hovmöller plot of the sea-level pressure (contours- mb) and the zonal component of the 10 m wind (color, m s^{-1}) along 147°W , indicated by the blue line in Figure 1a. The highs (H) and the lows (L) that resulted in strong easterly flow along the Beaufort Sea shelf, indicated by the blue lines, are labeled. The three transects occupied during the cruise are denoted by the blue dashed lines.

water has a strong shelf remineralization signature, with high inorganic nutrient concentrations and elevated CO_2 partial pressures ($p\text{CO}_2$) [Mathis *et al.*, 2007]. The current is readily reversed (flows westward) in response to easterly or northeasterly winds. Such winds can arise due a strengthening of the Beaufort Sea High [e.g., Watanabe, 2011], and/or the passage of Aleutian Low storms located far to the south [Pickart *et al.*, 2009a]. The offshore Ekman transport associated with the easterly winds induces upwelling of higher-salinity halocline waters from the boundary current and deep basin all along the shelfbreak [Pickart *et al.*, 2009b]. Reversals of the current are common during the storm season in autumn and winter: Nikolopoulos *et al.* [2009] found that the dominant velocity variability observed along the shelfbreak during this part of the year was due to such reversals. However, upwelling can occur throughout the year [Schulze and Pickart, 2011, also

Seasonal variation of upwelling in the Alaskan Beaufort Sea, submitted to *Journal of Geophysical Research*, 2012].

[5] Despite the prevalence of upwelling along the Beaufort shelfbreak, very little is known about how these events impact the carbon biogeochemistry of the water column due to a lack of direct observations. Here we describe the carbon chemistry of the shelf both before and during a storm event that occurred in October 2011. These new observations reveal some startling trends in carbonate mineral saturation states (Ω) and fluxes of CO_2 to the atmosphere.

2. Methods

[6] Direct observations of temperature, salinity, pH, total alkalinity (TA), dissolved inorganic carbon (DIC), and inorganic nutrients were made throughout the water column near the Beaufort Sea shelfbreak (Figure S1) in October of 2011 from the *USCGC Healy*. A seabird 911+ conductivity/temperature/depth (CTD) instrument was used, mounted on a 24-position 10-liter rosette. Partial gas pressure of CO_2 ($p\text{CO}_2$) was measured at the surface, with real-time mapping following the methods described by McNeil *et al.* [2005]. Water column $p\text{CO}_2$ and seawater calcium carbonate (CaCO_3) saturation states for aragonite (Ω_{arg}) and calcite (Ω_{cal}) were calculated from pH, TA, temperature, salinity, phosphate, and silicate data, using CO2SYS (version 1.05) and the thermodynamic model of Lewis and Wallace [1995]. Uncertainty in the calculation of Ω was <0.02 . The error for $p\text{CO}_2$ was $\sim 5\%$ of the total value. A more detailed description of the methods used here is included in the auxiliary material.

[7] Air-sea CO_2 fluxes (F_{CO_2} ; $\text{mmol m}^{-2} \text{d}^{-1}$) were determined from direct measurements of $p\text{CO}_2$ from the underway system using:

$$F_{\text{CO}_2} = F_{\text{SST}} \times F_{\text{CO}_2} \times \Delta p\text{CO}_2 \quad (1)$$

where k_{SST} is the gas transfer velocity (cm hr^{-1}), K_{CO_2} is the solubility of CO_2 ($\text{mmol m}^{-3} \mu\text{atm}^{-1}$) estimated by Weiss [1974], and $\Delta p\text{CO}_2$ is the air-sea $p\text{CO}_2$ difference (μatm). Values of k_{SST} were determined from the quadratic wind speed dependency from Ho *et al.* [2011], such that:

$$k_{\text{SST}} = (0.277 \times U_{10}^2) \times (\text{Sc}/600)^{-0.5} \quad (2)$$

where U_{10} is wind speed corrected to 10 m elevation above the sea surface, and Sc is the Schmidt number for CO_2 at the *in situ* temperature. Wind speed was measured from sensors mounted on the vessel. Hull-mounted acoustic Doppler current profiler (ADCP) velocities were processed using the CODAS software package [Firing, 1991] and subsequently de-tided using the Oregon State University Global Inverse Solution [Egbert *et al.*, 1994]. To assess the atmospheric conditions during the cruise, reanalysis fields from the National Centers for Atmospheric Prediction (NCEP) and the North American Regional Reanalysis (NARR) were analyzed. The high resolution (32 km, 3 hr) of the NARR [Mesinger *et al.*, 2006] makes it especially useful in this region.

[8] To determine the total CO_2 flux we assumed that upwelling formed quickly in response to wind-forcing. We considered two areas to determine the total flux during this

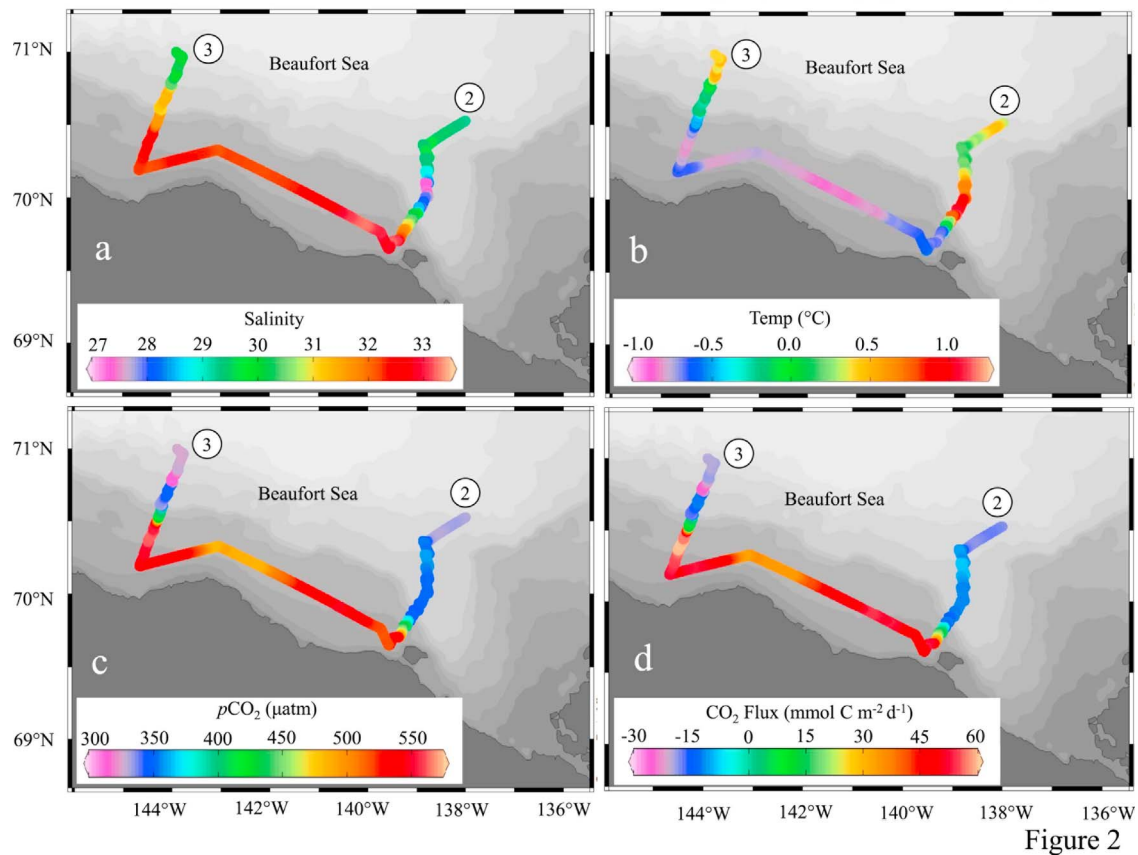


Figure 2

Figure 2. Data from the underway system at CTD lines 2 and 3 and a transect along the shelfbreak. (a) Salinity; (b) temp. ($^{\circ}\text{C}$); (c) $p\text{CO}_2$ (μatm); (d) CO_2 Flux ($\text{mmol C m}^{-2} \text{d}^{-1}$), a positive value means that the CO_2 flux is from the ocean to the atmosphere.

event. First, we took the area covered by our observations (5.5° longitude by 0.4° latitude or $\sim 3 \times 10^{10} \text{ m}^2$) to provide a conservative estimate. We then assumed that this event likely impacted the entire length of the Beaufort shelf, particularly since winds were even stronger to the west of our observations. Accordingly, we considered an area of 15° longitude and 0.4° latitude or $\sim 9 \times 10^{10} \text{ m}^2$ to determine the potential regional flux.

3. Upwelling Effects on Beaufort Shelf Air-Sea CO_2 Flux and Carbonate Chemistry

[9] The average winds over the Chukchi and Beaufort Seas during the month of October 2011 were more than one standard deviation stronger than the long-term (1979-present) climatology for that month (Figure 1a), and were predominantly easterly/northeasterly (i.e., upwelling favorable). This was due to a combination of a series of Aleutian low pressure systems passing to the south, along with fluctuations in the strength of the Beaufort Sea High (Figure 1b). Four Aleutian lows traversed the Gulf of Alaska during the month, but the largest wind event along the North Slope occurred during Oct 14–21 when the Beaufort Sea High strengthened in conjunction with the passage of an Aleutian low pressure system. The zonal wind speed during this event exceeded 10 m s^{-1} , which is more than enough to reverse the shelfbreak jet and drive upwelling in open water conditions [Schulze and Pickart, 2011].

[10] Transect 1 (Figure S1) was occupied in the western Beaufort Sea before the onset of the large wind event (Figure 1b). During this time the upper water column was stratified both on the shelf and over the shelfbreak. Water density was $24\text{--}25 \text{ kg m}^{-3}$ at the surface over the shelf and decreased slightly (to $<23.5 \text{ kg m}^{-3}$) over the Canada Basin. DIC and $p\text{CO}_2$ in the upper 30 m over the shelf and shelfbreak ranged from 1950 to 2060 $\mu\text{moles kg}^{-1}$ and 330 to 350 μatm . Calcite and aragonite were both supersaturated ($\Omega_{\text{cal}} > 1.6$ and $\Omega_{\text{arg}} > 1.0$) over the shelf and in the surface waters of the Canada Basin, but aragonite was undersaturated in the upper halocline waters (100–175 m) over the Canada Basin.

[11] During the occupation of transect 1 the boundary current was flowing to the east ($>25 \text{ cm s}^{-1}$), centered at a depth of $\sim 100 \text{ m}$. The flow was bottom-intensified with a definitive biogeochemical signature of remnant winter Pacific water with DIC concentrations $>2200 \mu\text{moles kg}^{-1}$ and $p\text{CO}_2 > 600 \mu\text{atm}$. The temperature and salinity in the core of the current were -1.5°C and 32.5, respectively, with a density of 26.2 kg m^{-3} . Aragonite was undersaturated ($\Omega_{\text{arg}} < 0.8$) and calcite was close to undersaturation ($\Omega_{\text{cal}} < 1.2$) within the boundary current. The fact that the current was flowing eastward, along with the lack of an upwelling signature in the hydrographic fields, indicates that this transect sampled the undisturbed circulation at the shelf and shelfbreak.

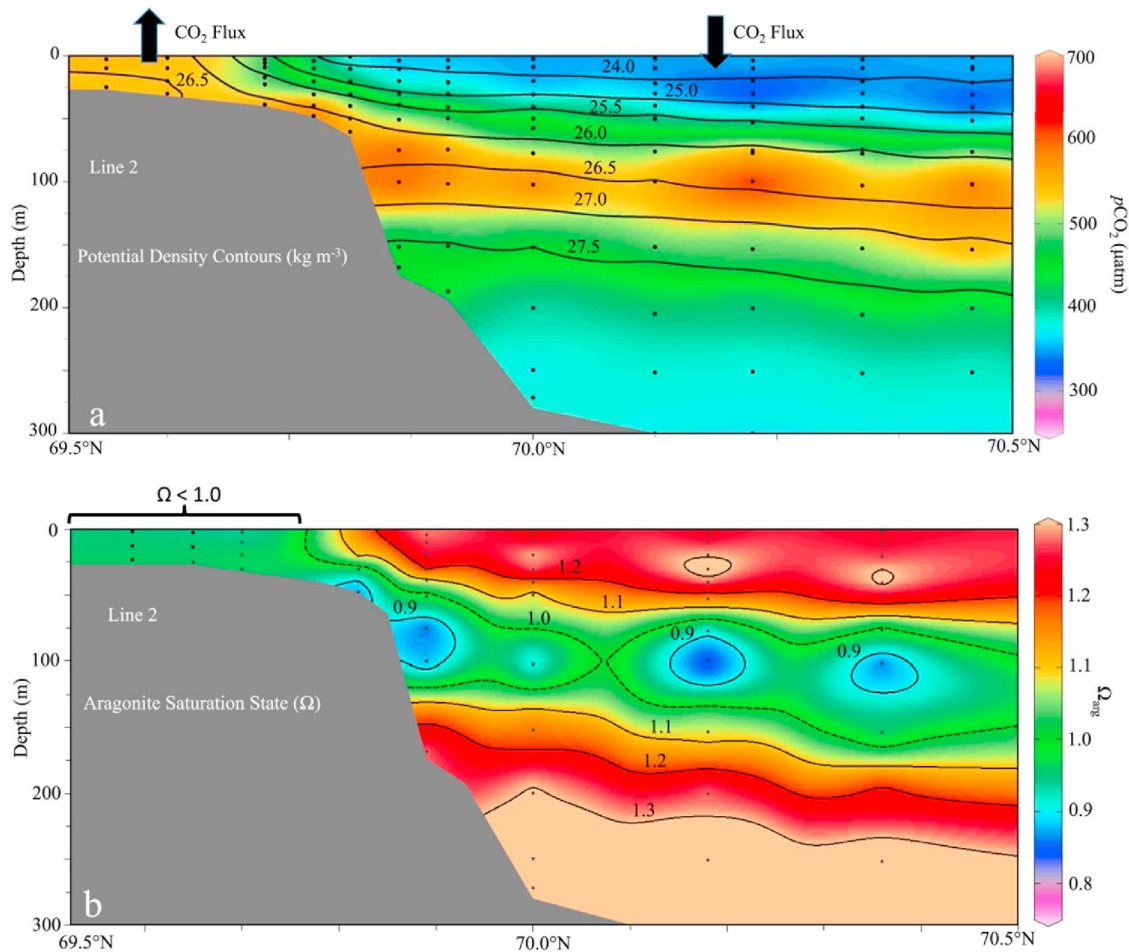


Figure 3. (a) Cross-sectional plot of $p\text{CO}_2$ (μatm) with density (kg m^{-3}) contours along CTD line 2. The black arrows indicate the direction of the CO_2 flux. (b) Cross-sectional plot of aragonite saturation state (Ω), with contour lines along CTD line 2. The dashed line illustrates where $\Omega = 1$.

[12] Roughly 10 days later, two transects that included underway $p\text{CO}_2$ sampling (Lines 2 and 3; Figure S1) were conducted to the east. Line 2 was near the Mackenzie River Delta, and Line 3 was roughly 200 km west of the delta. As seen in Figure 1b, these transects were occupied near the end of the 10-day storm event, and locally the ship measured winds exceeding 15 m s^{-1} from the east–northeast. In both transects the boundary current was reversed with surface-intensified flow exceeding 40 cm s^{-1} , and isopycnals were sloped upwards towards the shelf – the classic signature of upwelling [Pickart *et al.*, 2011]. The associated offshore Ekman flow in the upper layer had fluxed low salinity (<28.0), relatively warm ($>1.0^\circ\text{C}$) shelf water into the Canada Basin (Figure 2). This was in sharp contrast to the conditions we observed along transect 1 before the onset of strong winds from the east. Therefore, we consider our occupation of transect 1 to be a “before” picture of the shelf and shelf break when upwelling was not occurring.

[13] At the two eastern transects, the water on the shelf was replaced by deeper water upwelled from the basin. Since vigorous mixing takes place during this process, the water brought from depth was not identical to that of the undisturbed boundary current, but nonetheless it was quite distinct from the resident shelf water, which was warmer, had lower salinity and $p\text{CO}_2$, and higher Ω_{arg} . Consequently, a sharp

shelf-to-basin gradient was established in numerous properties, including temperature, salinity, density, and $p\text{CO}_2$. For example, the fresher water that was transported offshore had much lower $p\text{CO}_2$ ($\sim 350 \mu\text{atm}$) relative to the water that was upwelled from the boundary current ($\sim 550 \mu\text{atm}$) (Figures 2 and 3a).

[14] The upwelling event also had a pronounced effect on carbonate mineral saturation states both on and off the shelf. The low-salinity shelf water that was transported offshore was relatively replete in carbonate, such that $\Omega_{\text{arg}} > 1.2$ (Figure 3b) and $\Omega_{\text{cal}} > 2.0$. However, the upwelled waters were undersaturated with respect to aragonite ($\Omega_{\text{arg}} < 1.0$, Figure 3b) and low with respect to calcite saturation ($\Omega_{\text{cal}} < 2.0$). In light of the large zonal extent of the enhanced winds (Figure 1a), the upwelling of boundary current water likely caused aragonite undersaturation in the water column along the entire coast of the Beaufort Shelf (and perhaps the northeast Chukchi shelf as well).

[15] The presence of water supersaturated with respect to atmospheric $p\text{CO}_2$ at the sea surface, along with the enhanced wind speeds, created an outgassing event (Figure 2). Fluxes of CO_2 out of the water were on the order of $28\text{--}53 \text{ mmol C m}^{-2} \text{ d}^{-1}$ for hundreds of kilometers along the coast. This outgassing was slightly offset by the uptake of CO_2 by the waters transported offshore (-7 to

–14 mmol C m⁻² d⁻¹). The NARR fields indicate that the winds exceeded 8 m s⁻¹ for nearly 10 days during the strong event in the middle of the month (corroborated by the shipboard wind measurements). This implies a net outgassing of 0.18–0.54 Tg-C, or approximately 25% of the CO₂ taken up by the entire Beaufort Sea in an average year via primary productivity.

[16] Due to the prevalence of Aleutian lows and their associated tracks during the autumn and winter months [e.g., *Favorite et al.*, 1976], upwelling events are common in the Beaufort Sea. Indeed, over the two year period from 2002–4, 45 such events were measured by a mooring array situated across the shelf/slope near the location of transect 1 [*Schulze and Pickart*, 2011]. Furthermore, upwelling occurred even in the presence of 100% ice cover. However, when ice is present much of the CO₂ flux to the atmosphere would be mitigated by the ice barrier to air–sea exchange. Therefore, while upwelling events in the presence of ice would likely bring waters undersaturated with respect to aragonite onto the shelf, the CO₂ outgassing would be limited. Accordingly, pCO₂ supersaturations and carbonate mineral undersaturations would be preserved on the shelf for longer periods of time. Currently, the ice in this region of the Beaufort Sea is returning later each year and is thinning, both of which could lead to long-term enhancement of CO₂ outgassing in the region.

[17] Using an estimate of 4 open water upwelling events per year [*Schulze and Pickart*, 2011], implies an annual outgassing of 0.72–2.16 Tg-C, or roughly 2–24% of the annual estimated sink for CO₂ on the Chukchi Shelf [i.e., *Bates et al.*, 2011]. It should be noted, however, that the time period studied by *Schulze and Pickart* [2011] was characterized by a weakened Beaufort Sea High [*von Appen and Pickart*, 2012], which is less favorable for upwelling. Since the late 2000s the Beaufort Sea High has strengthened, and the modeling study of *Watanabe* [2011] suggests that under such enhanced easterly winds the shelfbreak jet is significantly weakened and offshore Ekman transport is the dominant mode of shelf-basin exchange. This suggests that the outgassing CO₂ flux estimate given above may be conservative, which is also supported by the notion that more high latitude storms are predicted under a warming climate [*Zhang et al.*, 2004; *Sorteberg and Walsh*, 2008]. Consequently, the Beaufort Sea may be a source of CO₂ to the atmosphere, and play a greater role in the regional carbon budget, than previously thought.

4. Conclusions

[18] Data from a recently observed upwelling event in the Beaufort Sea has provided valuable new insights into major controls on water column carbon biogeochemistry. When this shelf is forced by easterly winds due to the passage of Aleutian lows to the south and/or a strengthened Beaufort Sea High, boundary current water that is replete in CO₂ and undersaturated in aragonite is upwelled to the surface. The net effect of this upwelling is an outgassing of CO₂ to the atmosphere and the dispersal of water that is potentially corrosive to carbonate-shelled organisms over the shelf. Since these upwelling events are natural occurrences, it is likely that this part of the western Arctic shelf has always been a larger source of CO₂ to the atmosphere than has previously been assumed. However, recent reduction in sea

ice extent and duration, coupled with increased storm activity, has likely exacerbated the impacts of upwelling on water column saturation states and CO₂ flux across the air–sea interface. Upwelling of this undersaturated water onto the shelf is yet another potential stressor for both benthic and pelagic calcifying organisms in the western Arctic Ocean.

[19] **Acknowledgments.** The authors would like to thank the officers and crew of the *USCGC Healy* for their dedicated and unwavering support of our work. Funding for this work was provided by the National Science Foundation (ARC1041102 – JTM, OPP0856244-RSP, and ARC1040694-LWJ), the National Oceanic and Atmospheric Administration (CIFAR11021-RHB) and the West Coast & Polar Regions Undersea Research Center (POFP00983 – CLM and JM). McNeil is Vice President and co-owner of Pro-Oceanus Systems, Inc. manufacturer of the pCO₂ sensor used in this study.

[20] The Editor thanks two anonymous reviewers for their assistance in evaluating this paper.

References

- Anderson, L. G., and S. Kaitin (2001), Carbon fluxes in the Arctic Ocean: Potential impact by climate change, *Polar Res.*, 20(2), 225–232, doi:10.1111/j.1751-8369.2001.tb00060.x.
- Bates, N. R., W.-J. Cai, and J. T. Mathis (2011), The ocean carbon cycle in the western Arctic Ocean: Distributions and air–sea fluxes of carbon dioxide, *Oceanography*, 24(3), 186–201, doi:10.5670/oceanog.2011.71.
- Carmack, E., and R. W. Macdonald (2002), Oceanography of the Canadian Shelf of the Beaufort Sea: A setting for marine life, *Arctic*, 55, Suppl. 1, 29–45.
- Carmack, E., and P. Wassmann (2006), Food webs and physical-biological coupling on pan-Arctic shelves: Unifying concepts and comprehensive perspectives, *Prog. Oceanogr.*, 71, 446–477, doi:10.1016/j.pocean.2006.10.004.
- Egbert, G. D., A. F. Bennett, and M. G. G. Foreman (1994), TOPEX/POSEIDON tides estimated using a global inverse model, *J. Geophys. Res.*, 99(C12), 24,821–24,852, doi:10.1029/94JC01894.
- Favorite, F., A. J. Dodimead, and K. Nasu (1976), Oceanography of the subarctic Pacific region, 1960–71, *Bull. 33*, 187 pp., Int. North Pac. Fish. Comm., Vancouver, B. C., Canada.
- Firing, E. (1991), Acoustic Doppler current profiling methods and navigation. WOCE Hydrographic Program Operations and Methods Manual, *WHP Off. Rep. WHPO 91-1*, *WOCE Rep. 68/91*, Woods Hole Oceanogr. Inst., Woods Hole, Mass.
- Ho, D. T., R. Wanninkhof, P. Schlosser, D. S. Ullman, D. Hebert, and K. F. Sullivan (2011), Toward a universal relationship between wind speed and gas exchange: Gas transfer velocities measured with ³He/SF₆ during the Southern Ocean Gas Exchange Experiment, *J. Geophys. Res.*, 116, C00F04, doi:10.1029/2010JC006854.
- Lewis, E. R., and D. W. R. Wallace (1995), Basic programs for the CO₂ system in seawater, *Rep. BNL-61827*, Brookhaven Natl. Lab., Upton, N. Y.
- Macdonald, R. W., L. G. Anderson, J. P. Christensen, L. A. Miller, I. P. Semiletov, and R. Stein (2010), Polar margins: The Arctic Ocean, in *Carbon and Nutrient Fluxes in Continental Margins: A Global Synthesis*, edited by K. K. Liu et al., pp. 291–303, Springer, New York.
- Mathis, J. T., R. S. Pickart, D. A. Hansell, D. Kadko, and N. R. Bates (2007), Eddy transport of organic carbon and nutrients from the Chukchi Shelf: Impact on the upper halocline of the western Arctic Ocean, *J. Geophys. Res.*, 112, C05011, doi:10.1029/2006JC003899.
- Mathis, J. T., N. R. Bates, D. A. Hansell, and T. Babila (2009), Interannual variability of net community production over the northeast Chukchi Sea shelf, *Deep Sea Res., Part II*, 56, 1213–1222, doi:10.1016/j.dsr2.2008.10.017.
- McNeil, C., D. Katz, R. Wanninkhof, and B. Johnson (2005), Continuous shipboard sampling of gas tension, oxygen and nitrogen, *Deep Sea Res., Part I*, 52, 1767–1785, doi:10.1016/j.dsr.2005.04.003.
- Mesinger, F., et al. (2006), North American regional reanalysis, *Bull. Am. Meteorol. Soc.*, 87, 343–360, doi:10.1175/BAMS-87-3-343.
- Nikolopoulos, A., R. S. Pickart, P. S. Fratantoni, K. Shimada, D. J. Torres, and E. P. Jones (2009), The western Arctic boundary current at 152°W: Structure, variability, and transport, *Deep Sea Res., Part II*, 56, 1164–1181, doi:10.1016/j.dsr2.2008.10.014.
- Pickart, R. S., G. W. K. Moore, A. M. Macdonald, I. A. Renfrew, J. E. Walsh, and W. S. Kessler (2009a), Seasonal evolution of Aleutian low-pressure systems: Implications for the North Pacific sub-polar circulation, *J. Phys. Oceanogr.*, 39, 1317–1339, doi:10.1175/2008JPO3891.1.

- Pickart, R. S., G. W. K. Moore, D. J. Torres, P. S. Fratantoni, R. A. Goldsmith, and J. Yang (2009b), Upwelling on the continental slope of the Alaskan Beaufort Sea: Storms, ice, and oceanographic response, *J. Geophys. Res.*, *114*, C00A13, doi:10.1029/2008JC005009.
- Pickart, R. S., M. A. Spall, G. W. K. Moore, T. J. Weingartner, R. A. Woodgate, K. Aagaard, and K. Shimada (2011), Upwelling in the Alaskan Beaufort Sea: Atmospheric forcing and local versus non-local response, *Prog. Oceanogr.*, *88*, 78–100, doi:10.1016/j.pocean.2010.11.005.
- Sabine, C. L., et al. (2004), The oceanic sink for anthropogenic CO₂, *Science*, *305*, 367–371, doi:10.1126/science.1097403.
- Schulze, L. M., and R. S. Pickart (2011), Wind-forced upwelling on the continental slope of the Alaskan Beaufort Sea, paper presented at the 11th Conference on Polar Meteorology and Oceanography, Am. Meteorol. Soc., Boston, Mass., 2–5 May.
- Serreze, M. C., and J. A. Francis (2006), The Arctic amplification debate, *Clim. Change*, *76*, 241–264, doi:10.1007/s10584-005-9017-y.
- Sorteberg, A., and J. E. Walsh (2008), Seasonal cyclone variability at 70°N and its impact on moisture transport into the Arctic, *Tellus, Ser. A*, *60*(3), 570–586, doi:10.1111/j.1600-0870.2008.00314.x.
- von Appen, W.-J., and R. S. Pickart (2012), Two configurations of the western Arctic shelfbreak current in summer, *J. Phys. Oceanogr.*, doi:10.1175/JPO-D-11-026.1, in press.
- Wang, M. Y., and J. E. Overland (2009), A sea-ice free summer Arctic within 30 years?, *Geophys. Res. Lett.*, *36*, L07502, doi:10.1029/2009GL037820.
- Watanabe, E. (2011), Beaufort shelfbreak eddies and shelf-basin exchange of Pacific summer water in the western Arctic Ocean detected by satellite and modeling analyses, *J. Geophys. Res.*, *116*, C08034, doi:10.1029/2010JC006259.
- Weingartner, T. J., D. J. Cavalieri, K. Aagaard, and Y. Sasaki (1998), Circulation, dense water formation, and outflow on the northeast Chukchi shelf, *J. Geophys. Res.*, *103*, 7647–7661, doi:10.1029/98JC00374.
- Weiss, R. F. (1974), Carbon dioxide in water and seawater: The solubility of a non-ideal gas, *Mar. Chem.*, *2*, 203–215, doi:10.1016/0304-4203(74)90015-2.
- Zhang, X., J. E. Walsh, J. Zhang, U. S. Bhatt, and M. Ikeda (2004), Climatology and interannual variability of Arctic cyclone activity: 1948–2002, *J. Clim.*, *17*, 2300–2317, doi:10.1175/1520-0442(2004)017<2300:CAIVOA>2.0.CO;2.

F. Bahr and R. S. Pickart, Woods Hole Oceanographic Institution, Mail Stop 21, Woods Hole, MA 02543, USA.

R. H. Byrne, R. A. Easley, M. M. Elliot, X. Liu, and J. Ma, College of Marine Science, University of South Florida, 140 7th Ave. S., St. Petersburg, FL 33701, USA.

J. N. Cross, J. T. Mathis, and S. C. Reisdorph, School of Fisheries and Ocean Sciences, University of Alaska Fairbanks, 905 N. Koyukuk Dr., 245 O'Neill Bldg., Fairbanks, AK 99775, USA. (jmathis@sfos.uaf.edu)

R. A. Feely, Pacific Marine Environmental Laboratory, 7600 Sand Point Way NE, Seattle, WA 98115, USA.

L. W. Juranek, College of Oceanic and Atmospheric Sciences, Oregon State University, 104 CEOAS Admin. Bldg., Corvallis, OR 97331, USA.

T. Lichendorf, C. L. McNeil, and J. Morison, Applied Physics Laboratory, University of Washington, 1013 NE 40th St., Seattle, WA 98105, USA.

G. W. K. Moore, Department of Physics, University of Toronto, 60 St. George St., Toronto, ON M5S 1A7, Canada.